Supporting Information

Tune the coordination behavior of an unexplored asymmetric multidentate ligand for developing diverse heterometallic architectures with luminescent and magnetic properties

Xue-Qin, Song[a]*, Xue-Li Xia[a] , Fu-Qiang Song[a], Guo-Hua Liu[a], Li Wang[b,c]*

a) School of Chemical and Biological Engineering, Lanzhou Jiaotong University, Lanzhou 730070, China

b) College of Chemistry and Chemical Engineering. College of Chemistry and Chemical Engineering, Xi'an Shiyou University, Xi'an 710065, P.R. China.

c)State Key Laboratory of Coordination Chemistry, School of Chemistry and Chemical Engin eering, Nanjing University, Nanjing 210093, P.R. China

Contents

1. Materials and General Methods.

All chemicals were obtained from commercial vendors without further purification.

Elemental analyses of carbon, hydrogen and nitrogen were conducted on an Elementar Vario EL III analyzer. Infrared spectra (4000~400 cm^{-1}) were obtained with KBr discs on a Therrno Mattson FTIR spectrometer. Thermogravimetric and differential thermal analysis experiments were performed using a TGA/NETZSCH STA449C instrument heated from 25~650 °C (heating rate of 10 °C/min, nitrogen stream). X-ray powder diffraction (XRPD) patterns of the samples were recorded on a X-ray diffractometer (Rigaku D/Max 2200PC) in the 2θ range from 5° to 50° at room temperature. Simulation of the PXRD pattern was carried out with the single-crystal X-ray diffraction data (SXRD) using Mercury software (version: 3.10). Emission and excitation spectra in visible region were recorded with a Hitachi F-7000 spectrophotometer equipped with quartz cuvettes of 1 cm path length. Luminescence measurements were performed using a 2.5 nm × 2.5 nm slit width. Luminescence measurements of NIR emission as well as lifetime measurements were carried out on an Edinburgh FLS920 phosphorimeter equipped with a continuous Xe-900 xenon lamp. The absolute emission quantum yields of the compounds were measured at room temperature using a calibrated integrating sphere as a sample chamber, and specpure $BaSO_4$ was used as a reflecting standard. Direct-current (dc) magnetic susceptibility measurements were carried out on a Quantum Design SQUID MPMS-XL 7 magnetometer operating between 2 and 300 K for dc applied fields at 1000 Oe. Field dependence of the magnetization at 2~10K magnetic susceptibility measurements on the polycrystalline samples were performed with the same magnetometer at different magnetic fields. The data were corrected for the magnetization of the sample holder and the diamagnetism of the constituent atoms using Pascal constants. All crystalline samples characterized by PXRD, TG, EA, IR, photoluminescence and magnetic studies were obtained from the same batch.

2. Synthesis of H_3L.

The ligand **H_3L** was prepared according to the procedures outlined in the literature using 2-hydroxy-1,3-propylenediamine to replace ethaneamine.[1] Yield: 76%. Melting point: 192~194 ℃. Elem anal. Calcd for $C_{19}H_{22}N_2O_6$: C, 60.95; H, 5.92; N, 7.48. Found: C, 61.28; H, 5.96; N, 7.50. ^{1}H NMR (500 MHz, DMSO-d_6) δ 13.79 (s, 1H), 12.70 (s, 1H), 8.73 (t, *J* = 5.4 Hz, 1H), 8.06 (s, 1H), 7.49 – 7.43 (m, 1H), 7.02 (d, *J* = 8.0 Hz, 1H), 6.95 (d, J = 7.9 Hz, 2H), 6.77 (dt, *J* = 9.3, 8.2 Hz,

2H), 4.03 (d, J = 5.0 Hz, 1H), 3.83 (d, J = 2.3 Hz, 7H), 3.77 (dd, J = 12.4, 4.0 Hz, 1H), 3.64 – 3.51 (m, 2H), 3.44 – 3.34 (m, 1H). IR(KBr, υ, cm^{-1})： 3452(w), 1636(s), 1543(s), 1470(s), 1374(m), 1253 (m), 1087(m), 734 (m).

3. Synthesis of Zn_8Ln_2: 0.1 mmol (37 mg) **H_3L** and 0.20 mmol NEt_3 (27 μL) were dissolved in 21 mL CH_3CN to obtain a clear yellow CH_3CN solution, then 0.1 mmol (18 mg) $Zn(OAc)_2{\cdot}2H_2O$ was added to afford a pale yellow suspension. After further stirring for 2 hours, 7 mL CH_3OH was added droply to result a clear solution in which 0.1 mmol $Ln(OAc)_3{\cdot}6H_2O$ was added. The mixture was stirred overnight, filtered into a sealed 10~20 mL glass vial and set aside for slow evaporation. After about one month, pale yellow single crystals suitable for crystal analysis were obtained which were collected by filtration, washed with cold methanol, and dried in the air.

$[Zn_8Nd_2L_2(OH)_4(OAc)_{12}]{\cdot}2CH_3OH{\cdot}2H_2O$ (**Zn_8Nd_2**) Yield: 55 mg, 45% based on **H_3L**. Elemental analysis for $C_{64}H_{90}N_4Nd_2O_{44}Zn_8$: Calcd.: C 31.62; H 3.73; N 2.30. Found: C 31.72, H 3.75, N 2.28. IR (KBr, υ, cm^{-1}): 3451 (m), 1602 (s), 1554 (s), 1444 (s), 1219 (s), 1081 (m), 852 (m), 742 (m).

$[Zn_8Tb_2L_2(OH)_4(OAc)_{12}]{\cdot}CH_3OH{\cdot}CH_3CN$ (**Zn_8Tb_2**) Yield: 60 mg, 49% based on **H_3L**. Elemental analysis for $C_{65}H_{85}N_5O_{41}Tb_2Zn_8$: Calcd.: C 32.08; H 3.52; N 2.88. Found: C 32.48, H 3.54, N 2.85. .IR (KBr, υ, cm^{-1}): 3449 (m), 1597 (s), 1553 (s), 1443(s), 1219 (s), 1078 (m), 852 (m), 742 (m).

$[Zn_8Dy_2L_2(OH)_4(OAc)_{12}]{\cdot}CH_3OH{\cdot}CH_3CN$ (**Zn_8Dy_2**) Yield: 64 mg, 53% based on **H_3L**. Elemental analysis for $C_{65}H_{85}Dy_2N_4O_{41}Zn_8$: Calcd.: C 38.76; H 3.43; N 8.48. Found: C 38.58, H 3.42, N 8.50. IR (KBr, υ, cm^{-1}): 3449 (m), 1598 (s), 1553 (s), 1445(s), 1221 (s), 1080 (m), 853 (m), 744 (m).

$[Zn_8Er_2L_2(OH)_4(OAc)_{12}]{\cdot}2CH_3CN$ (**Zn_8Er_2**) Yield: 62 mg, 51% based on **H_3L**. Elemental analysis for $C_{66}H_{84}Er_2N_6O_{39}Zn_8$: Calcd.: C 32.45; H 3.47; N 3.44. Found: C 32.48, H 3.46, N 3.42. IR (KBr, υ, cm^{-1}): 3449 (m), 1601 (s), 1553 (s), 1443 (s), 1223 (s), 1080 (m), 852 (m), 742 (m).

4. Synthesis of Ni_3Tb_2 A similar procedure as that for preparation of **Zn_8Tb_2** was employed by replacing of $Zn(OAc)_2{\cdot}2H_2O$ with $Ni(OAc){\cdot}2H_2O$. $[Ni_3Tb_2(HL)_2(OH)_2(OAc)_6]{\cdot}3CH_3CN{\cdot}H_2O$, Yield: 52 mg, 58% based on **H_3L**. Elemental analysis for $C_{56}H_{71}N_7Ni_3O_{27}Tb_2$: Calcd.: C 38.04; H 4.05; N 5.55. Found: C 38.29, H 4.03, N 5.59. IR (KBr, υ, cm^{-1}): 3419 (m), 1624 (s), 1559 (s), 1454 (s), 1409 (s), 1313 (m), 1220 (m), 1073 (m), 853 (m), 744 (m).

5. Synthesis of Ni_2Tb_2: A similar procedure as that for preparation of **Ni_3Tb_2** was adopted by using $Tb(NO_3)_3 \cdot 6H_2O$ as a lanthanide source. $[Ni_2Tb_2(HL)_2(OAc)_4(NO_3)_2(H_2O)_2] \cdot 4CH_3CN \cdot 3H_2O$, Yield: 40 mg, 45% based on **H_3L**. Elemental analysis for $C_{54}H_{74}N_{10}Ni_2O_{31}Tb_2$: calcd.: C 36.14, H 4.16, N 7.81, found: C 36.19, H 4.15, N 7.78. IR (KBr, υ, cm^{-1}): 3424 (m), 1627 (s), 1575 (s), 1476 (s), 1454 (s), 1409 (s), 1217 (s), 1070 (m), 1028 (m), 852 (m), 744 (m).

6. Details of Single Crystal X-ray Diffraction

X-ray Data Collection and Reduction. Suitable block crystals of **Zn_8Nd_2**, **Zn_8Tb_2**, **Zn_8Dy_2**, **Zn_8Er_2**, **Ni_3Tb_2** and **Ni_2Tb_2** were coated with perfluoropolyether oil before mounting. Intensity data for the aligned crystals of **Zn_8Tb_2**, **Zn_8Dy_2**, **Zn_8Er_2**, **Ni_3Tb_2** and **Ni_2Tb_2** were recorded at 293(2) K and that of **Zn_8Nd_2** and **Ni_3Tb_2** were recorded at 173 (2) K by employing a Bruker SMART APEX II CCD diffractometer. Mo Kα radiation (λ= 0.71073 Å) source were adopted for **Zn_8Nd_2**, **Zn_8Tb_2**, **Zn_8Dy_2** and **Ni_2Tb** and Cu Kα radiation (λ= 1.54184 Å) were used for **Zn_8Er_2** and **Ni_3Tb_2**. No crystal decay was observed during the data collections. The frames were integrated with the Bruker SAINT software package using a narrowframe algorithm. Data were corrected for absorption effects using the empirical multiscan method (SADABS).[2]

Structure Solution and Refinement. The structures were solved by direct methods and refined on F^2 by a full-matrix least-squares procedure. SHELXL-2014/2016 was used for both structure solutions and refinements.[3] The locations of the heaviest atoms were determined easily. The O, N, and C atoms were subsequently determined from the difference Fourier maps and refined anisotropically. The H atoms were incorporated at calculated positions and refined with fixed geometry and riding thermal parameters with respect to their carrier atoms. Crystallographic diagrams were drawn using the DIAMOND software package.[4] Also severely disordered solvents molecules in **Zn_8Tb_2**, **Zn_8Dy_2**, **Ni_3Tb_2** and **Ni_2Tb_2** were removed by SQUEEZE during the structural refinements.[5] For details about the squeezed material, see cif data in Supporting Information. Therefore, solvent molecules which were determined on the basis of elemental microanalysis, thermal analysis and the data treated with the SQUEEZE routine within PLATON were added to the molecular formula of **Zn_8Tb_2**, **Zn_8Dy_2**, **Ni_3Tb_2** and **Ni_2Tb_2** respectively.

Table S1. Selected bond lengths (Å) for **Zn_8Nd_2**, **Zn_8Tb_2**, **Zn_8Dy_2**, **Zn_8Er_2**, **Ni_3Tb_2** and **Ni_2Tb_2**.

$[Zn_8Nd_2L_2(OH)_4(OAc)_{12}]\cdot CH_3OH\cdot H_2O$ (**Zn_8Nd_2**)										
Nd1–O1	2.714(4)	Nd1–O2	2.401(4)	Nd1–O4	2.431(4)	Nd1–O5	2.432(4)	Nd1–O7	2.515(3)	
Nd1–O8	2.505(3)	Nd1–O13	1.595(4)	Nd1–O15	2.418(4)	Nd1–O17	2.419(3)	Zn1–O3	1.936(3)	
Zn1–O7	1.940(3)	Zn1–O16	1.954(3)	Zn1–O19	2.024(3)	Zn2–N1	2.048(4)	Zn2–O2	2.034(3)	
Zn2–O3	2.058(3)	Zn2–O7	2.018(3)	Zn2–O20	2.033(4)	Zn3–O5	2.023(4)	Zn3–O6	2.219(4)	
Zn3–O8	2.040(3)	Zn3–O9	1.982(4)	Zn3–O14	1.962(4)	Zn4–O8	1.940(3)	Zn4–O10	1.986(4)	
Zn4–O12	1.920(4)	Zn4–O18	1.939(4)							
$[Zn_8Tb_2L_2(OH)_4(OAc)_{12}]\cdot CH_3OH\cdot CH_3CN$ (**Zn_8Tb_2**)										
Tb1–O1	2.715(6)	Tb1–O2	2.451(6)	Tb1–O4	2.470(5)	Tb1–O5	2.481(6)	Tb1–O10	2.474(6)	
Tb1–O12	2.602(6)	Tb1–O17	2.469(6)	Tb1–O19	2.551(5)	Tb1–O20	2.572(5)	Zn1–O3	1.923(5)	
Zn1–O7	2.012(5)	Zn1–O9	1.953(6)	Zn1–O20	1.937(5)	Zn2–N1	2.037(7)	Zn2–O2	2.032(5)	
Zn2–O3	2.058(5)	Zn2–O8	2.027(6)	Zn2–O20	2.010(5)	Zn3–O5	2.012(5)	Zn3–O6	2.212(6)	
Zn3–O11	1.960(6)	Zn3–O13	1.973(6)	Zn3–O19	2.030(5)	Zn4–O14	1.982(7)	Zn4–O16	1.917(6)	
Zn4–O18	1.941(6)	Zn4–O19	1.929(6)							
$[Zn_8Dy_2L_2(OH)_4(OAc)_{12}]\cdot CH_3OH\cdot CH_3CN$ (**Zn_8Dy_2**)										
Dy1–O1	2.715(5)	Dy1–O2	2.415(5)	Dy1–O4	2.444(5)	Dy1–O5	2.433(5)	Dy1–O10	2.438(5)	
Dy1–O11	2.531(4)	Dy1–O13	2.632(5)	Dy1–O19	2.440(4)	Dy1–O20	2.527(4)	Zn1–O3	1.941(4)	
Zn1–O8	2.017(5)	Zn1–O9	1.958(4)	Zn1–O11	1.950(4)	Zn2–N1	2.041(6)	Zn2– O2	2.041(4)	
Zn2– O3	2.056(4)	Zn2–O7	2.036(5)	Zn2–O11	2.014(4)	Zn3–O5	2.032(5)	Zn3–O6	2.203(6)	
Zn3–O12	1.964(6)	Zn3–O14	1.979(5)	Zn3–O20	2.030(5)	Zn4–O15	1.994(5)	Zn4–O16	1.933(5)	
Zn4–O18	1.949(5)	Zn4–O20	1.947(4)							
$[Zn_8Er_2L_2(OH)_4(OAc)_{12}]\cdot 2CH_3CN$ (**Zn_8Er_2**)										
Er1–O2	2.343(6)	Er1–O3	2.387(5)	Er1–O5	2.300(5)	Er1–O6	2.711(5)	Er1–O8	2.349(5)	
Er1–O9	2.590(6)	Er1–O16	2.323(5)	Er1–O19	2.411(5)	Er1–O20	2.432(4)	Zn1–O1	2.247(7)	
Zn1–O2	2.033(5)	Zn1–O10	1.953(6)	Zn1–O11	2.000(6)	Zn1–O19	2.062(5)	Zn2–N2	2.034(6)	
Zn2–O4	2.057(4)	Zn2–O5	2.047(4)	Zn2–O7	2.053(5)	Zn2–O20	2.010(4)	Zn3–O12	1.990(8)	
Zn3–O13	1.941(7)	Zn3–O15	1.954(7)	Zn3–O19	1.931(5)	Zn4–O4	1.923(4)	Zn4–O17	2.028(5)	
Zn4–O18	1.965(5)	Zn4–O20	1.939(4)							
$[Ni_3Tb_2(HL)_2(OH)_2(OAc)_6]\cdot 3CH_3CN\cdot H_2O$ (**Ni_3Tb_2**)										
Tb1–O1	2.533(3)	Tb1–O2	2.292(3)	Tb1–O7	2.659(3)	Tb1–O8	2.309(3)	Tb1–O13	2.319(3)	
Tb1–O15	2.311(3)	Tb1–O24	2.381(3)	Tb1–O25	2.357(3)	Tb2–O5	2.321(3)	Tb2–O6	2.648(3)	
Tb2–O11	2.289(3)	Tb2–O12	2.616(3)	Tb2–O18	2.386(3)	Tb2–O20	2.286(3)	Tb2–O22	2.300(3)	
Tb2–O26	2.348(3)	Ni1–N2	2.008(4)	Ni1–O4	2.103(3)	Ni1–O5	2.000(3)	Ni1–O19	2.108(3)	
Ni1–O23	2.091(3)	Ni1–O26	2.018(3)	Ni2–O16	2.065(3)	Ni2–O18	2.115(3)	Ni2–O21	2.071(3)	
Ni2–O24	2.125(3)	Ni2–O25	2.008(3)	Ni2–O26	2.001(3)	Ni3–N3	2.007(4)	Ni3–O8	2.004(3)	
Ni3–O9	2.121(3)	Ni3–O14	2.104(3)	Ni3–O17	2.091(3)	Ni3–O25	2.010(3)			
$[Ni_2Tb_2(HL)_2(OAc)_4(NO_3)_2(H_2O)_2]\cdot 4CH_3CN\cdot 3H_2O$ (**Ni_2Tb_2**)										
Tb1–O1	2.638(4)	Tb1–O2	2.297(4)	Tb1–O5	2.347(4)	Tb1–O6	2.498(4)	Tb1–O7	2.426(4)	
Tb1–O8	2.402(4)	Tb1–O9	2.361(4)	Tb1–O11	2.456(5)	Tb1–O12	2.500(5)	Ni1–N1	2.042(5)	
Ni1–O2	2.010(4)	Ni1–O4	2.030(4)	Ni1–O5	2.020(4)	Ni1–O10	2.101(4)	Ni1–O14	2.080(5)	

S H A P E v2.1 Continuous Shape Measures calculation

(c) 2013 Electronic Structure Group, Universitat de Barcelona Contact: llunell@ub.edu

---

Table S2 Shape calculation of Ln^{III} in **Zn_8Nd_2**, **Zn_8Tb_2**, **Zn_8Dy_2**, **Zn_8Er_2**, **Ni_3Tb_2** and **Ni_2Tb_2**.

	Zn_8Nd_2	**Zn_8Tb_2**	**Zn_8Dy_2**	**Zn_8Er_2**	**Ni_3Tb_2**		**Ni_2Tb_2**
Enneagon (EP-9)	0.2010	0.1973	0.2007	0.2558	–	–	0.2203
Octagonal pyramid (OPY-9)	0.1318	0.1341	0.1329	0.1387	–	–	0.2112
Heptagonal bipyramid (HBPY-9)	0.2222	0.2273	0.2260	0.2146	–	–	0.2251
Johnson triangular cupola J3 (JTC-9)	0.1752	0.1727	0.1751	0.1771	–	–	0.1779
Capped cube J8 (JCCU-9)	0.1675	0.1669	0.1659	0.1628	–	–	0.1254
Spherical-relaxed capped cube (CCU-9)	0.1785	0.1786	0.1779	0.1641	–	–	0.1579
Capped square antiprism J10 (JCSAPR-9)	0.1138	0.1184	0.1168	0.0973	–	–	0.1427
Spherical capped square antiprism (CSAPR-9)	0.1074	0.1107	0.1096	0.0932	–	–	0.1675
Tricapped trigonal prism J51 (JTCTPR-9)	0.1098	0.1135	0.1104	0.0926	–	–	0.1496
Spherical tricapped trigonal prism (TCTPR-9)	0.1050	0.1079	0.1081	0.9790	–	–	0.1692
Tridiminished icosahedron J63 (JTDIC-9)	0.1762	0.1736	0.1760	0.1643	–	–	0.1899
Hula-hoop (HH-9)	0.1790	0.1806	0.1804	0.1686	–	–	0.1480
Muffin (MFF-9)	0.1007	0.1031	0.1024	0.0893	–	–	0.1534
Octagon (OP-8)	–	–	–	–	0.2259	0.2565	–
Heptagonal pyramid (HPY-8)	–	–	–	–	0.1882	0.2053	–
Hexagonal bipyramid (BPY-8)	–	–	–	–	0.1892	0.2016	–
Cube (CU-8)	–	–	–	–	0.1895	0.2004	–
Square antiprism (SAPR-8)	–	–	–	–	0.0778	0.0973	–
Triangular dodecahedron (TDD-8)	–	–	–	–	0.0793	0.0874	–
Johnson gyrobifastigium (JGBF-8)	–	–	–	–	0.1559	0.1774	–
Johnson elongated triangular bipyramid (JETBPY-8)	–	–	–	–	0.1947	0.2072	–
Biaugmented trigonal prism J50 (JBTPR-8)	–	–	–	–	0.0626	0.0693	–
Biaugmented trigonal prism (BTPR-8)	–	–	–	–	0.0764	0.0763	–
Snub diphenoid J84 (JSD-8)	–	–	–	–	0.0740	0.0886	–
Triakis tetrahedron (TT-8)	–	–	–	–	0.1907	0.2049	–
Elongated trigonal bipyramid (ETBPY-8)	–	–	–	–	0.1805	0.2260	–

Table S3. H-bond parameters in $\mathbf{Zn_8Nd_2}$, $\mathbf{Ni_3Tb_2}$ and $\mathbf{Ni_2Tb_2}$.

Complex	D–H···A	*d*(D–H)	*d*(H···A)	*d*(D···A)	∠D–H···A	Symmetry code
$\mathbf{Zn_8Nd_2}$	N2–H2···O21	0.859(5)	2.008(1)	2.844(9)	164.43(2)	1-x, 2-y, 2-z
	O21–H21···O11	0.821(2)	1.909(3)	2.687(3)	157.70(6)	1-x, 1.5+y, 2.5-z
	O22–H22B···O11	0.875(3)	1.942(4)	2.799(2)	165.77(3)	1-x, 1.5+y, 2.5-z
	O22–H22B···O8	0.750(2)	2.006(7)	2.753(9)	173.97(0)	1-x, 1.5+y, 2.5-z
$\mathbf{Ni_3Tb_2}$	O9–H9···O10	0.862(1)	1.948(3)	2.709(4)	146.49(4)	2-x, 1-y, 1-z
	O4–H4B···O3	0.887(8)	1.851(7)	2.696(2)	158.16(9)	1-x, -y, -z
	O27–H27B···O3	0.849(8)	2.237(4)	3.035(5)	156.45(9)	1-x, -y, -z
	O26–H26···O27	0.980(2)	2.044(3)	2.959(9)	154.69(4)	x, y, z
$\mathbf{Ni_2Tb_2}$	N2–H2···O3	0.861(3)	2.068(8)	2.858(8)	152.20(2)	1-x, 1-y, 1- z
	O14–H14A···O15	0.855(3)	1.854(5)	2.687(6)	164.2(1)	1-x, 1-y, 1- z
	O15–H15A···O7	0.809(9)	1.996(1)	2.761(9)	157.50(6)	1-x, 1-y, 1- z
	O15–H15B···O8	0.819(6)	1.974(8)	2.787(2)	171.02(8)	-0.5+x,1.5 -y, 0.5+z

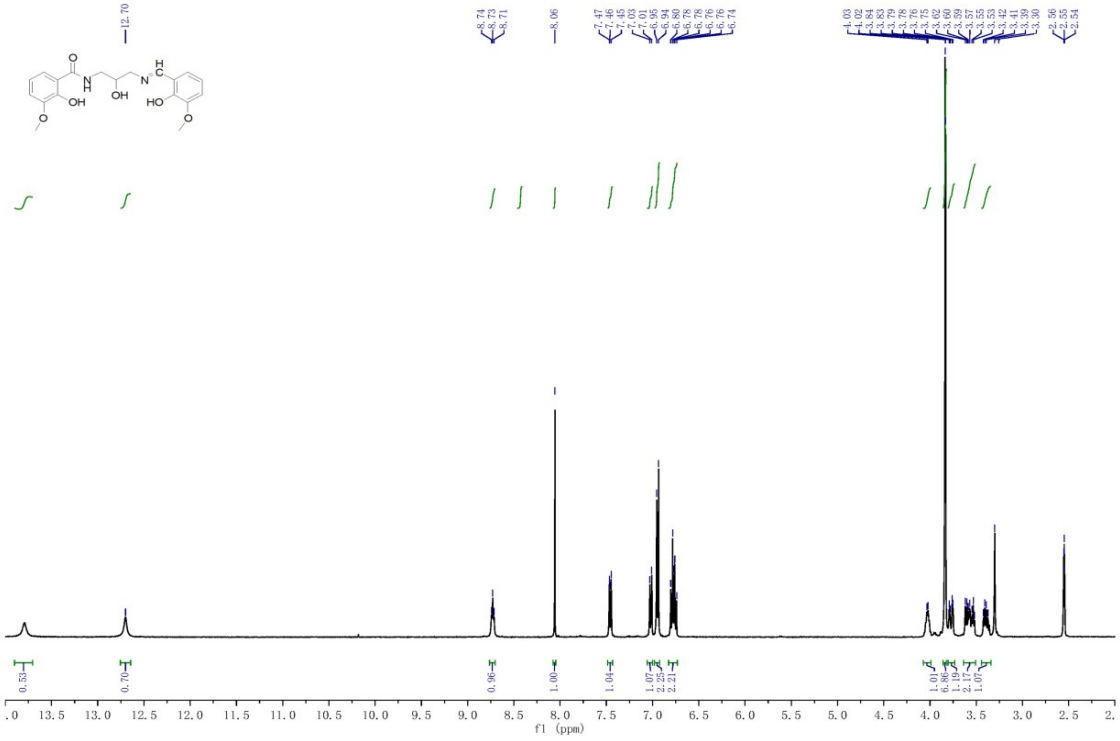

Figure S1. ^{1}H NMR spectra of $\mathbf{H_3L}$ in d_6-DMSO.

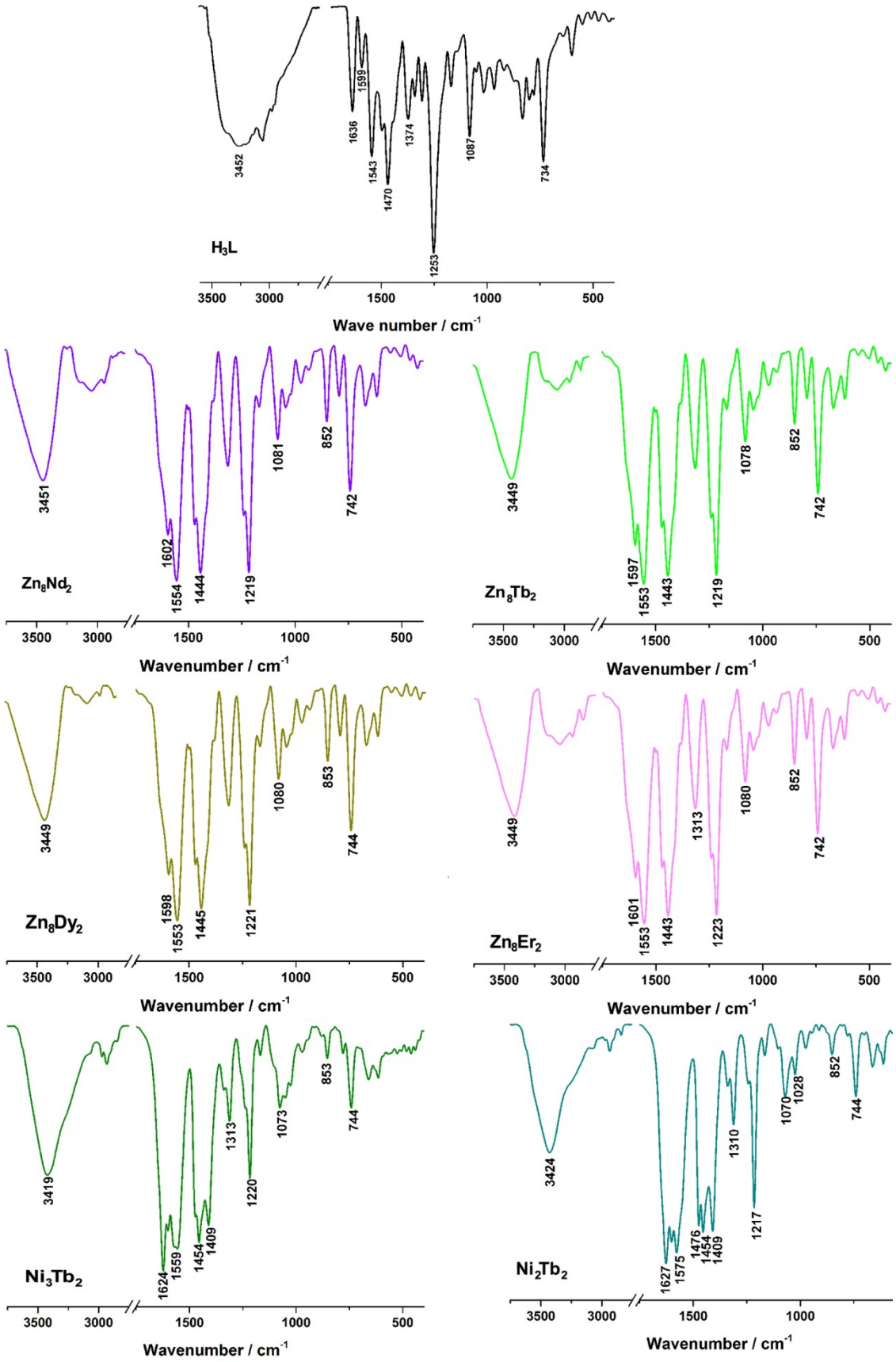

Figure S2. IR spectra of H_3L, Zn_8Nd_2, Zn_8Tb_2, Zn_8Dy_2, Zn_8Er_2, Ni_3Tb_2 and Ni_2Tb_2 in solid state.

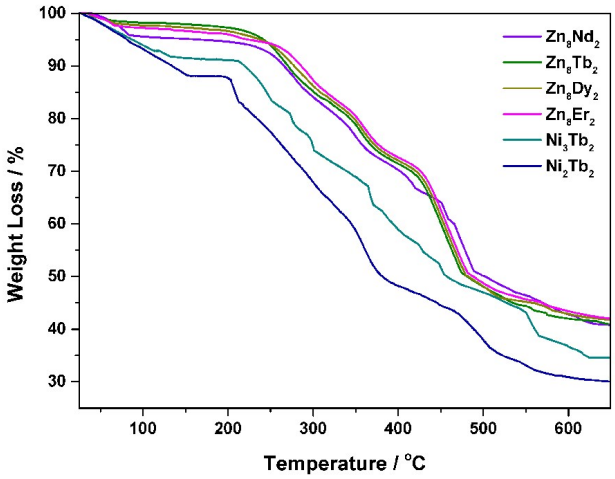

Figure S3. TGA curves of Zn_8Nd_2, Zn_8Tb_2, Zn_8Dy_2, Zn_8Er_2, Ni_3Tb_2 and Ni_2Tb_2 from 25 ~ 650 °C.

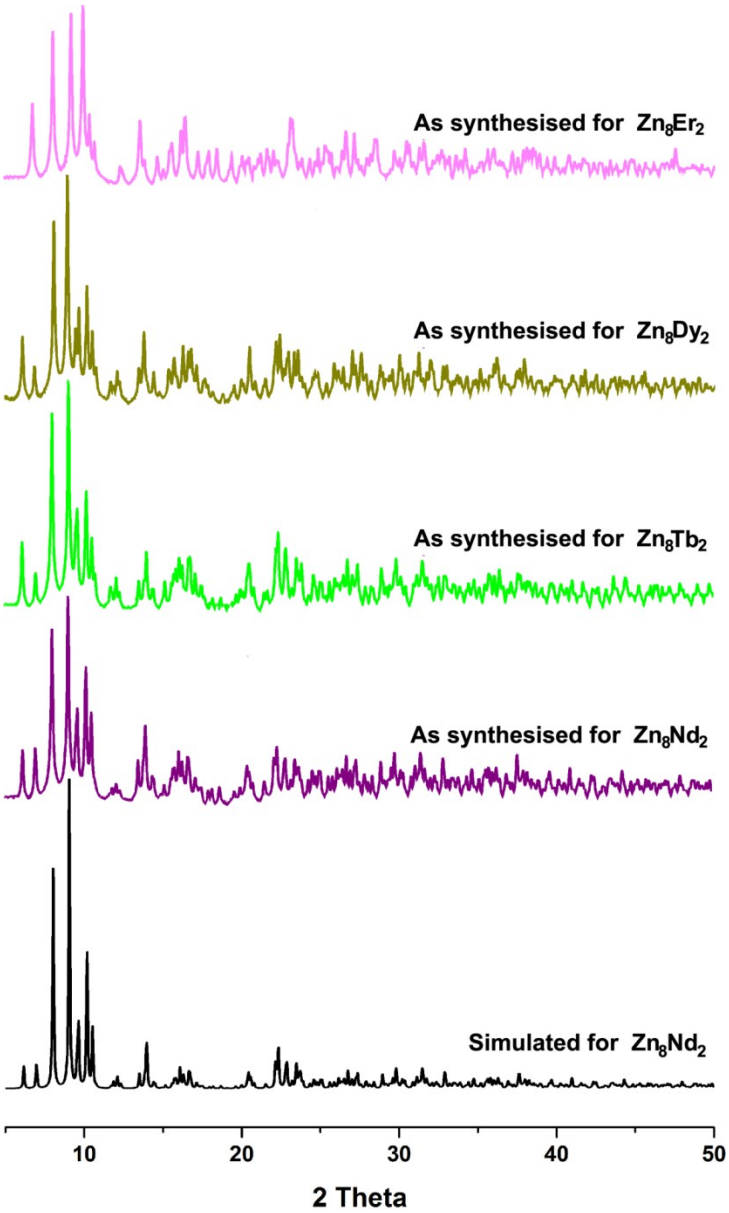

Figure S4. PXRD patterns of synthesized and simulated Zn_8Nd_2, Zn_8Tb_2, Zn_8Dy_2 and Zn_8Er_2.

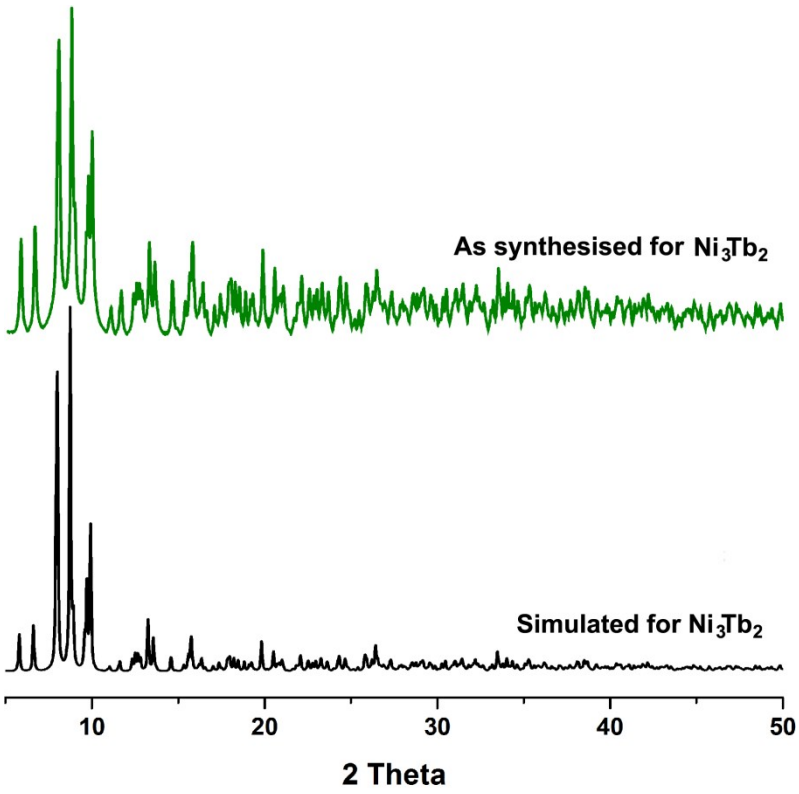

Figure S5. PXRD patterns of synthesized and simulated Ni_3Tb_2.

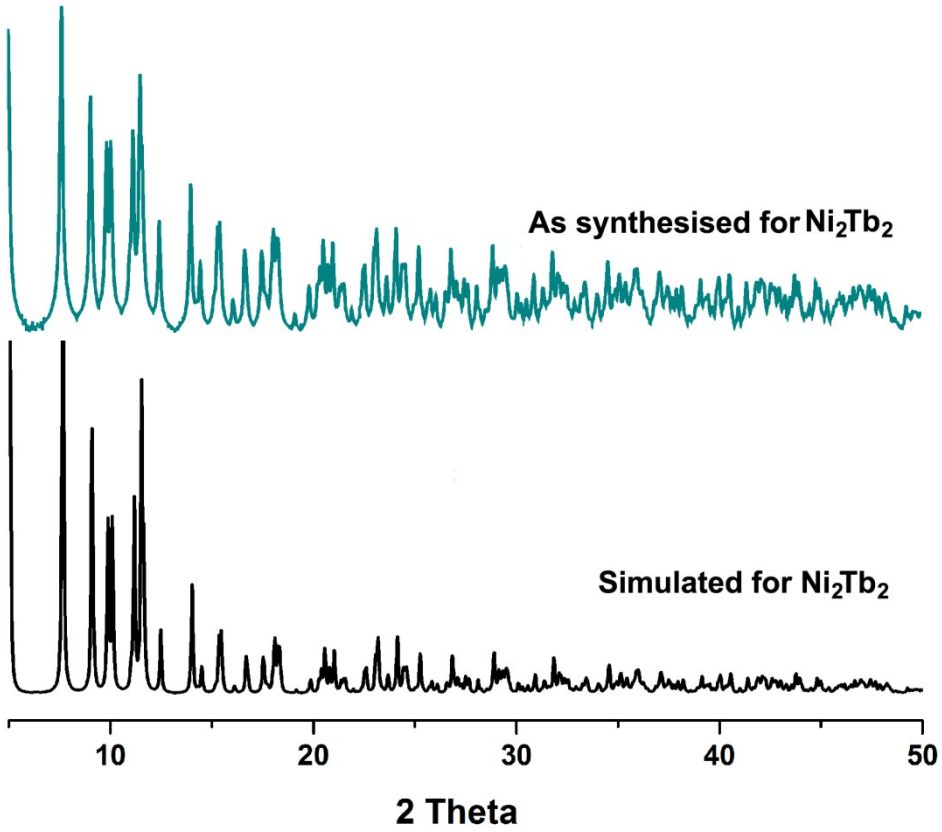

Figure S6. PXRD patterns of synthesized and simulated Ni_2Tb_2.

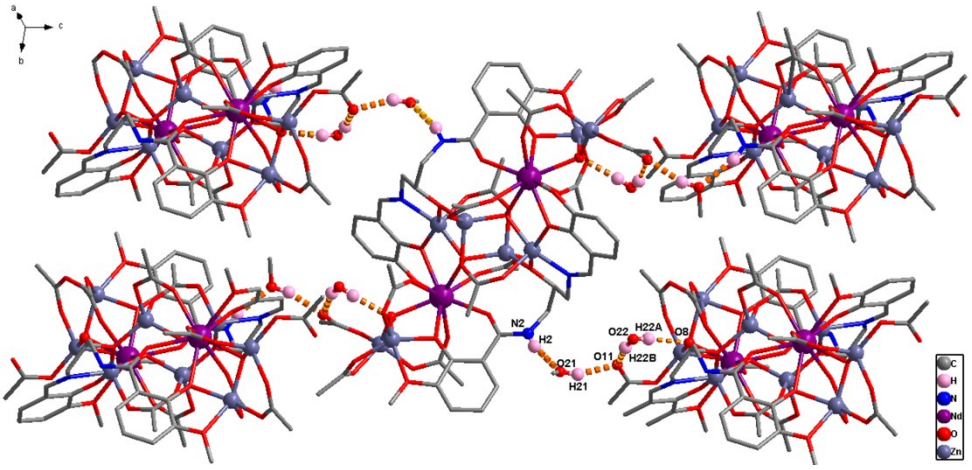

Figure S7 2D Supramolecular architecture of Zn_8Nd_2 constructed by intermolecular H-bond.

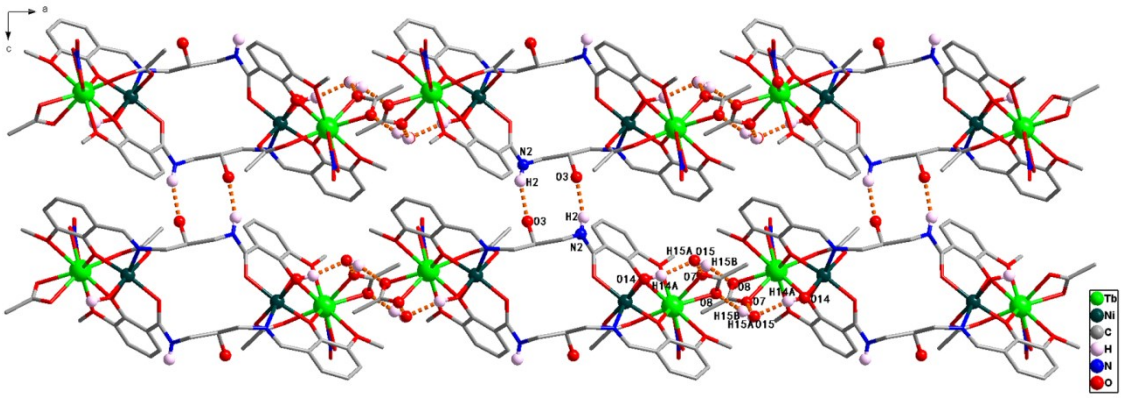

Figure S8 3D supramolecular network of Ni_2Tb_2 constructed by intermolecular H-bond viewing along b-axis.

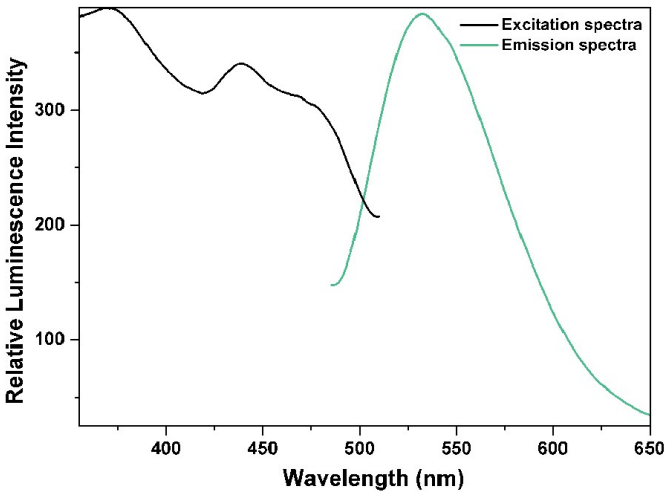

Figure S9 Excitation and emission spectra of H_3L in solid state.

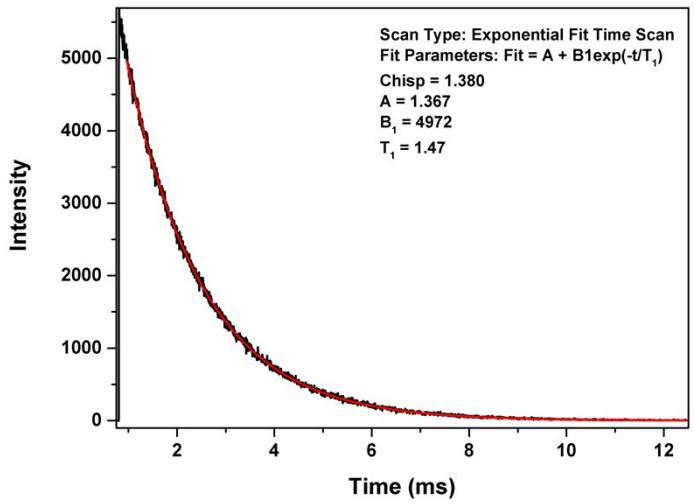

Figure S10 Emission intensity decay curves of $\mathbf{Zn_8Tb_2}$ in solid state monitored at 546 nm.

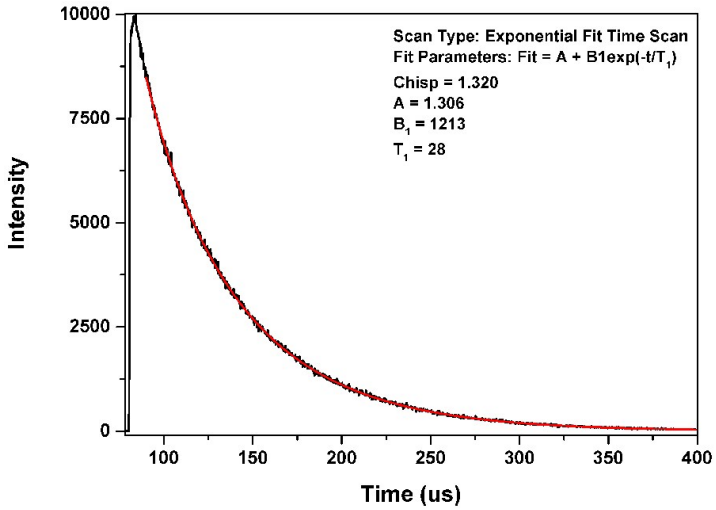

Figure S11 Emission intensity decay curves of $\mathbf{Zn_8Dy_2}$ in solid state monitored at 484 nm.

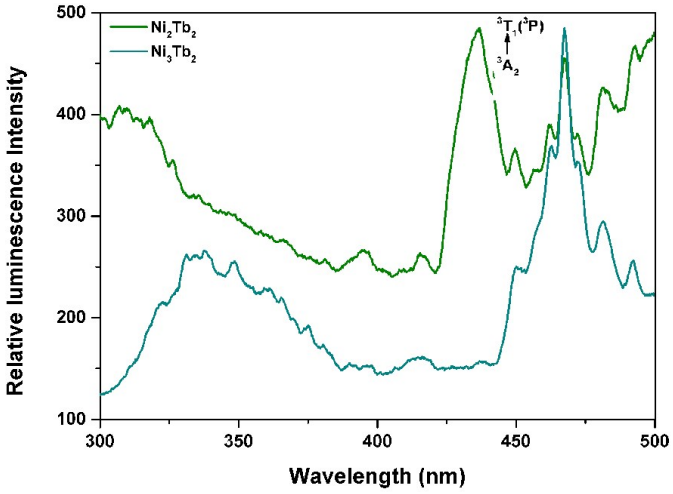

Figure S12 Excitation spectra of $\mathbf{Ni_3Tb_2}$ and $\mathbf{Ni_2Tb_2}$ monitored at 546 nm.

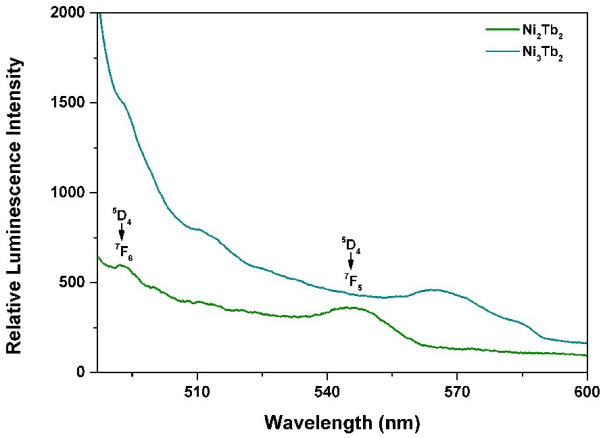

Figure S13 Emission spectra of Ni_3Tb_2 and Ni_2Tb_2 upon excited at 467nm.

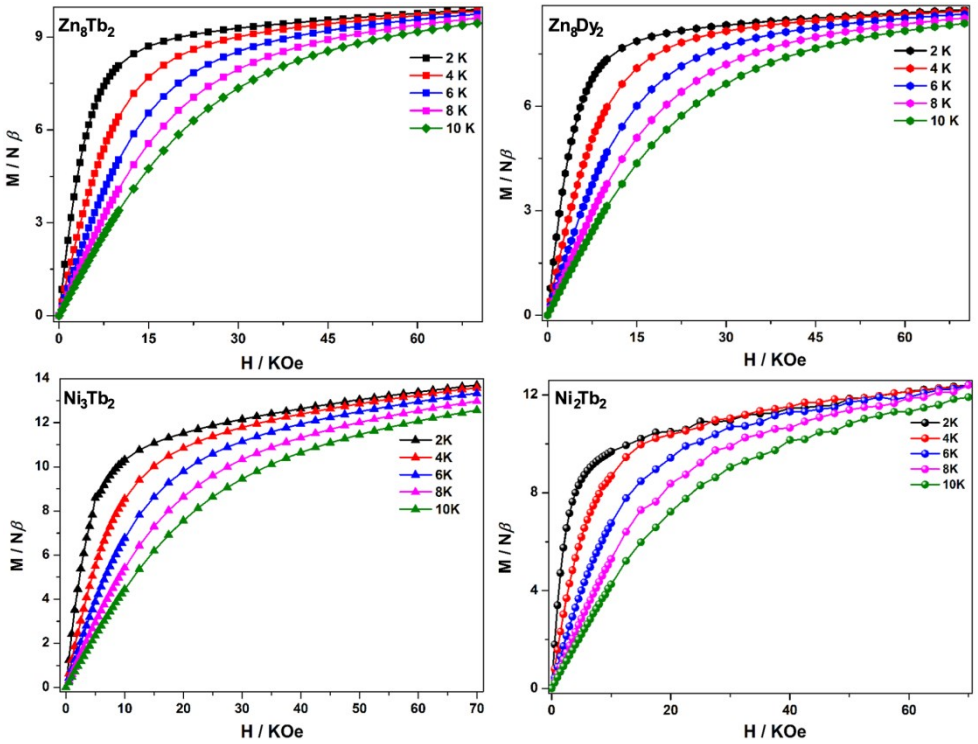

Figure S14 M-H curves of Zn_8Tb_2, Zn_8Dy_2, Ni_3Tb_2 and Ni_2Tb_2.

Reference

1 Y. -A. Liu, C. -Y.Wang, M.Zhang, X. -Q. Song, Polyhedron, 2017, *127*, 278-286.

2 SADABS, version 2.03; Bruker AXS Inc. Madison, WI, 2002.

3 G. M. Sheldrick, SHELXL-1997; University of Gottingen: Gottingen, Germany, 2014.

4 DIAMOND, Visual Crystal Structure Information System, version 3.1; Crystal Impact: Bonn, Germany, 2004.

5 A. L. Spek, The calculation of the solvent-accessible was performed by using the PLATON software (similarly herein after) *J. Appl. Crystallogr*. 2003, *36*, 7.